INFLOW TURBULENCE GENERATION

A project report submitted by

GOKUL S NAIR
ME14B109

Under the guidance of

Dr. Kameswararao Anupindi

in partial fulfilment of the requirements
for the award of the degree of

MASTER OF TECHNOLOGY
AND
BACHELOR OF TECHNOLOGY

TURBOMACHINES LABORATORY
DEPARTMENT OF MECHANICAL ENGINEERING
INDIAN INSTITUTE OF TECHOLOGY MADRAS
MAY 2019

CERTIFICATE

This is to certify that the project report titled "**INFLOW TURBULENCE GENERATION**" submitted by **GOKUL S NAIR (ME14B109)**, to Indian Institute of Technology Madras, for the award of **Master of Technology and Bachelor of Technology in Mechanical Engineering** is a bona fide record of work carried out by him. The content of this report, in full or in parts, have not been submitted to any other institute or University for the award of any degree or diploma.

Dr. Kameswararao Anupindi
Assistant Professor
Dept. of Mechanical Engineering
IIT Madras, 600036

Prof. N. Ramesh Babu
Head of the Department
Dept. of Mechanical Engineering
IIT Madras, 600036

Place: Chennai
Date:

ACKNOWLEDGEMENTS

I wish to express my sincere thanks and gratitude to my guide **Dr. Kameswararao Anupindi** for his invaluable guidance and support during my project work.

I wish to thank my labmates **Priyesh Kakka**, **Sourabh Jogee**, **Ravi Gupta** and **Bhanu Mitra Bulusu** for their help and support.

I wish to thank my parents for their help, support, encouraging, and calming words throughout my life,

I wish to thank my friends who have always been there for me throughout my life in the institute as a pillar of support helping me weather tough times cheerfully.

Gokul S Nair

TABLE OF CONTENTS

ACKNOWLEDGMENTS ii

ABBREVIATIONS v

NOTATION vi

ABSTRACT vii

1 INTRODUCTION AND METHODOLOGY 1

1.1 Introduction and Numerical Methodology
1.2 About OpenFOAM and solvers used
1.3 Motivation
1.4 Setup
1.5 Boundary and Inlet conditions

2. RANDOM FLUCTUATIONS: 10 PERCENT. 7

2.1 Introduction
2.2 Results

3. RANDOM FLUCTUATIONS: 20 PERCENT 13

3.1 Introduction
3.2 Results

4. 5 PERCENT FLUCTUTATIONS AND COMPARISONS 17

4.1 Introduction
4.2 Results

5. CONCLUDING REMARKS AND SCOPE FOR FUTURE WORK 21

5.1 Concluding Remarks

5.2 Grid Independence for LES

5.3 Synthetic Eddy Method and Divergence Free Synthetic Eddy Method

5.4 Digital Filter Method

ABBREVIATIONS

DNS	Direct Numerical Simulaions
LES	Large Eddy Simulations
PISO	Pressure Implicit Spliiting of Operator
RANS	Reynolds Averaged Navier Stokes
rms	Root Mean Square
SIMPLE	Semi-Implicit Pressure Linked Equations

NOTATIONS

d	Jet width
$\delta_{0.5}$	Jet half width
ν	Kinematic viscosity
R_{ij}	Reynolds stress tensor
τ_{ij}^{r}	Residual stress tensor

ABSTRACT

The turbulence characteristics of a plane jet is studied using OpenFOAM, at a Reynolds number of 3000. The random fluctuations inlet condition is studied for a plane jet and the turbulence characteristics are analysed, and compared with the literature. More advanced methods for Inflow turbulence generation, such as the Digital Filter Method, are discussed. The method of large eddy simulations(LES) is used, with the pimpleFoam solver of OpenFOAM which uses the PISO algorithm. The maximum Courant number is fixed at 0.7 and the time difference between different steps is changed accordingly to achieve this. The LES model used is the Smagorinsky model.

We simulate a jet with random fluctuations at the inlet with the magnitude of the random fluctuations equal to 5 percent,10 percent, and 20 percent of the inlet velocity. We average over multiple timesteps to get the mean velocities and the correlations. Thus averaged results are further averaged in the spanwise direction using the VISIT software. We also run a case with a finer mesh. The results obtained are compared with cases from literature

CHAPTER 1

INTRODUCTION AND METHODOLOGY

1.1 Introduction and Numerical Methodology

Turbulent flow is a pattern of fluid motion characterized by chaotic changes in pressure and flow velocity. This is due to the non-linear nature of the Navier Stokes equations.

Further complicating matters, analytical solutions to even the simplest of turbulent flows do not exist. Turbulence can be observed both in everyday phenomena, such as smoke from a fire or in fast flowing brooks as well as in engineering applications such as fluid flowing through a pipe or combustion inside an Internal Combustion Engine. Analytical solutions to the Navier Stokes equations are not easily obtained and thus one turns to the discipline of Computational Fluid Dynamics. Even here, we face a hiccup. The fine resolution and high nonlinearity of turbulent phenomena require us to use large grids which are computationally expensive. Thus, we turn to various methods to model the turbulent phenomenon, beginning with the Reynolds Averaged Navier Stokes (RANS) equations. The basic idea behind RANS is to decompose the instantaneous quantities into time averaged and fluctuating quantities. However, this results in the RANS Equations having some correlation quantities such as the Reynolds stress tensor $R_{ij} = \rho\overline{u_i'u_j'}$. To obtain equations containing only the mean velocity and pressure, we need to close the RANS equations by modelling the Reynolds stress term as a function of the mean flow. Prominent models that achieve this include the mixing length model (due to Prandtl) and the k-ε model (due to Spalding and Launder).

Another technique is to use Large Eddy Simulations (LES) which choose to ignore the smallest turbulent scales by low pass filtering of the Navier Stokes equations. This works better than the RANS method in capturing the stochastic nature of the eddies in various scales.

The LES filter removes small scales, and a filtered equation for a given variable is defined as[3]

$$\overline{\phi(\boldsymbol{x},t)} = \int_{-\infty}^{\infty}\int_{-\infty}^{\infty}\phi(\boldsymbol{r},\tau)G(\boldsymbol{x}-\boldsymbol{r},t-\tau)d\tau d\boldsymbol{r}$$

Where G is the filter convolution kernel.

The filter G will have cutoff length and time scales associated with it, which are usually denoted by Δ and τ_c respectively. Scales smaller than this are eliminated from the variable.

For incompressible flow, the filtered continuity and Navier-Stokes equations read:

$$\frac{\partial \bar{u}_i}{\partial x_i} = 0$$

$$\frac{\partial \bar{u}_i}{\partial t} + \frac{\partial}{\partial x_j}\left(\overline{u_i' u_j'}\right) = -\frac{1}{\rho}\frac{\partial \bar{p}}{\partial x_i} + \nu\frac{\partial}{\partial x_j}\left(\frac{\partial \bar{u}_i}{\partial x_j} + \frac{\partial \bar{u}_j}{\partial x_i}\right) = -\frac{1}{\rho}\frac{\partial \bar{p}}{\partial x_i} + 2\nu\frac{\partial}{\partial x_j}S_{ij}$$

Where $\bar{p}$ is the filtered pressure field and S_{ij} is the strain-rate tensor.

The filtered advection term $\overline{u_i' u_j'}$ can be written as:[11]

$$\overline{u_i' u_j'} = \tau_{ij}^r + \bar{u}_i\bar{u}_j$$

Where τ_{ij}^r is the residual stress tensor.

An important related idea is that of turbulent length scales and the energy cascade. Kolmogorov introduced the idea that the smallest length scales of turbulence are universal and that they only depend on ε (the rate of dissipation of the turbulence kinetic energy per unit mass) and ν (kinematic viscosity). According to the idea of energy cascading, energy is transferred from the largest scales, via intermediate scales called the inertial subrange, to the smallest scales, ie., the Kolmogorov scale. This idea was nicely put in the form of a poem by Lewis F. Richardson.

Big whirls have little whirls

that feed on their velocity,

And little whirls have lesser whirls

and so on to viscosity[2]

In Large eddy simulations, one cannot completely neglect the small scale information which is filtered out. It is considered through the method of sub-grid-scale(SGS) modelling. The simplest and earliest sub-grid-scale model is the Smagorinsky model.

In recent times, due to advancements in computing power, Direct Numerical Simulations (DNS) which resolve all the fine turbulent length scales, are also increasingly being adopted.

1.2 About OpenFOAM And Solvers Used:

OpenFOAM, which stands for Opensource Field Operation and Manipulation, is an opensource C++ toolbox providing numerical solvers and pre/postprocessing utilities for numerically solving various problems, including computational fluid dynamics. It is distributed exclusively under the GNU General Public License(GPL), thus giving users the freedom to modify it as they wish.

In this work, the PimpleFoam solver of OpenFOAM has been used. PimpleFoam uses the PIMPLE algorithm which is a combination of the PISO(Pressure Implicit with Splitting of Operator) and SIMPLE(Semi-Implicit Method for Pressure-Linked Equations). OpenFOAM's PimpleFoam allows the user to specify the maximum Courant number(C) and adjusts the difference between two timesteps dynamically to achieve this upper limit on Courant number. In this work, the maximum Courant number has been set at 0.7 in all simulations.

The basic structure of an OpenFOAM CFD case consists of three folders called 0, constant, and system. The 0 folder would contain the mesh(after it has been built), initial velocity profiles etc. The constant folder contains transport properties like viscosity, and turbulence properties(if relevant). The system folder contains details regarding the construction of the mesh, instructions during runtime, details for parallelisation(if used), and details regarding the solver used. Parallelisation(if used) is done via the OpenMPI technique. All cases in this

report have been run in parallel using 6 cores. The mesh is decomposed using the decomposePar command and reconstructed using the reconstructPar command.

Large Eddy Simulations are performed using pimpleFoam, and the Smagorinsky model is used. The Smagorinsky coefficients used are $c_e = 1.048$, $c_k = 0.04717$, $C_k = 0.094$, and $C_e = 1.048$.

VisIt is the software used to perform spanwise averaging of the various variables. VisIT was developed by the US Department of Energy(DOE) Advanced Simulation and Computing Initiative(ASCI).

ParaView is also used for visualisation and post-processing. ParaView was initially developed as a collaborative effort between Kitware, Inc. and the Los Alamos National Laboratory.

1.3 Motivation

In Computational Fluid Dynamic simulations of jets, channels, and similar flows, if one starts off with laminar flow as an inlet condition, the flow is likely to stay laminar or take a long time to transition to turbulence as there are no random fluctuations to trip the flow into a turbulent regime as exists under experimental conditions. Thus, one has to start with a laminar mean flow field that has superimposed random fluctuations. However, even then, sometimes the fluctuations could die down or take a relatively long time to transition to turbulence. Therefore, one tries to provide various innovative initial flow fields that kick start turbulence much faster and saves precious computing time.

One method to do this is to recycle a turbulent flow field from an already solved similar problem, called an auxiliary simulation. These methods are called flow recycling methods. Flow recycling methods are mainly of two types — Strong Recycling and Weak Recycling. In the strong recycling method, the flow field at one selected streamwise station of an auxiliary simulation is used to initiate the flow in the main simulation. However, recycling methods suffer from various drawbacks including the introduction of spurious periodicities which are not physical to the main simulation. The other major class of methods are synthetic turbulence methods. Synthetic turbulence methods include the Synthetic Random Fourier Method and the Synthetic Digital Filtering method among others. One can also make use of data collected from experiments using hot wire probes or Particle Image Velocimetry (PIV). [1]

In this report, we study the method of superimposed random fluctuations using Large Eddy Simulations and compare the results to experimental and DNS simulations as well as earlier LES simulations from the literature. We also briefly discuss other novel methods to provide initial flow fields to enhance the turbulent nature of the flow.

1.4 Setup:

A grid that is 0.36m in the x-direction, 0.15m in the y-direction, and 0.04m in the z-direction is used. A plane jet is considered. The width of the jet inlet is 0.01m. The mesh is non uniform, being finer closer to the inlet and closer to the jet. The mesh is divided into three blocks, stacked one on top of the other in the y-direction, each having 300, 50, and 20 cells in the x,y, and z directions respectively. The width of the middle block is the same as that of the jet. This ensures a much larger concentration of cells in the middle region of the jet. This results in a total number of 0.9 million cells. A finer mesh with 360, 60, and 24 cells in the respective directions per block has also been considered for one case. This mesh would have a total of 1.552 million cells.

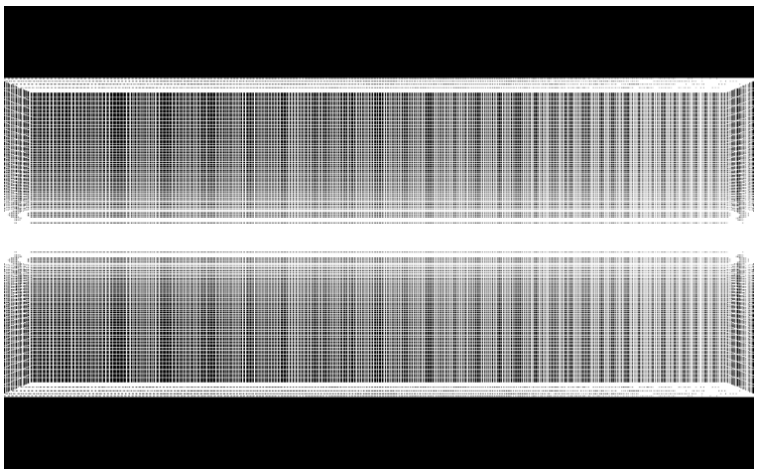

Figure 1.1: Mesh used

1.5 Boundary And Inlet Conditions:

Periodic boundary conditions are used for the z-direction. This allows one to approximate an infinite length in this direction using this mesh. Thus, the jet is, effectively, infinite in the z direction.

An advective boundary condition is used at the outlet, and a No-Slip boundary condition in the walls at the inlet.

The top and bottom walls have an entraining flow of velocity 0.013365. A velocity shear developing between this flow and the still fluid shall aid in generation of turbulence.

The inlet has a mean flow field of 0.2673 with turbulent fluctuations of varying magnitudes superimposed in each of the different cases studied.

CHAPTER 2

RANDOM FLUCTUATIONS 10%

2.1 Introduction:

In this case, the magnitude of the inlet fluctuations is equal to 10 percent of the plane inlet jet velocity. Both the velocity U and the fluctuation quantities reported here have been time averaged. The time averaging is done from t=6s to t=20s. The obtained time averaged quantities are further averaged in the spanwise direction using the ViSiT software.

2.2 Results:

The time and spanwise averaged velocity profile is shown in Figure 2.1

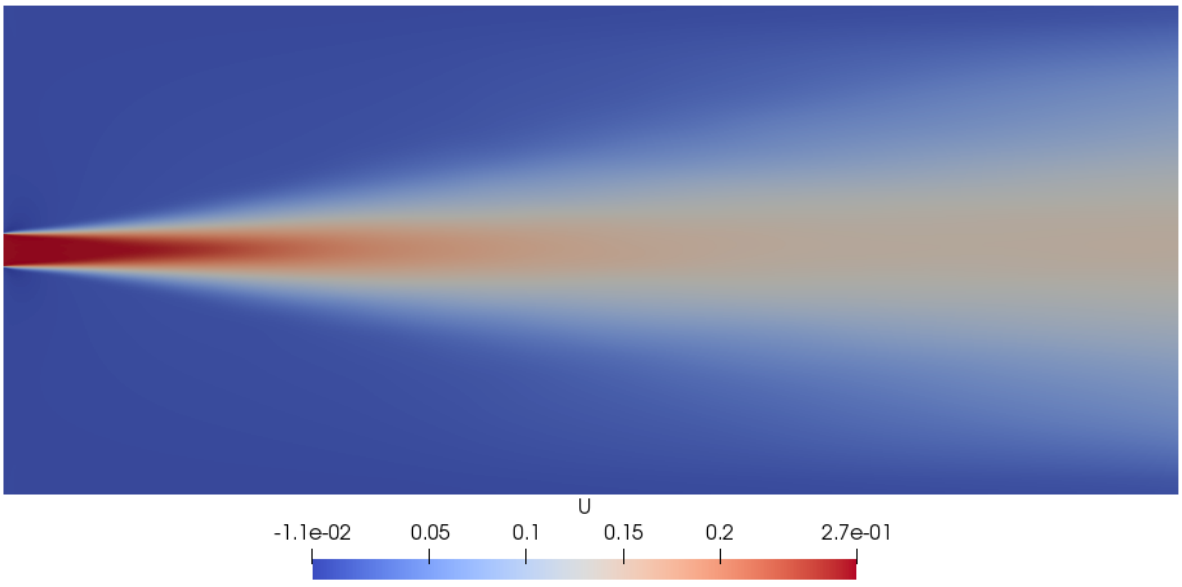

Figure 2.1: Time and spanwise averaged velocity profile

The time and spanwise averaged profiles of $< u'u' >$ and $< u'v' >$ are shown in Figures 2.2 and 2.3 respectively. $< u'u' >$ is found to be symmetrical about the centreline, with peaks a small distance away from the centreline.

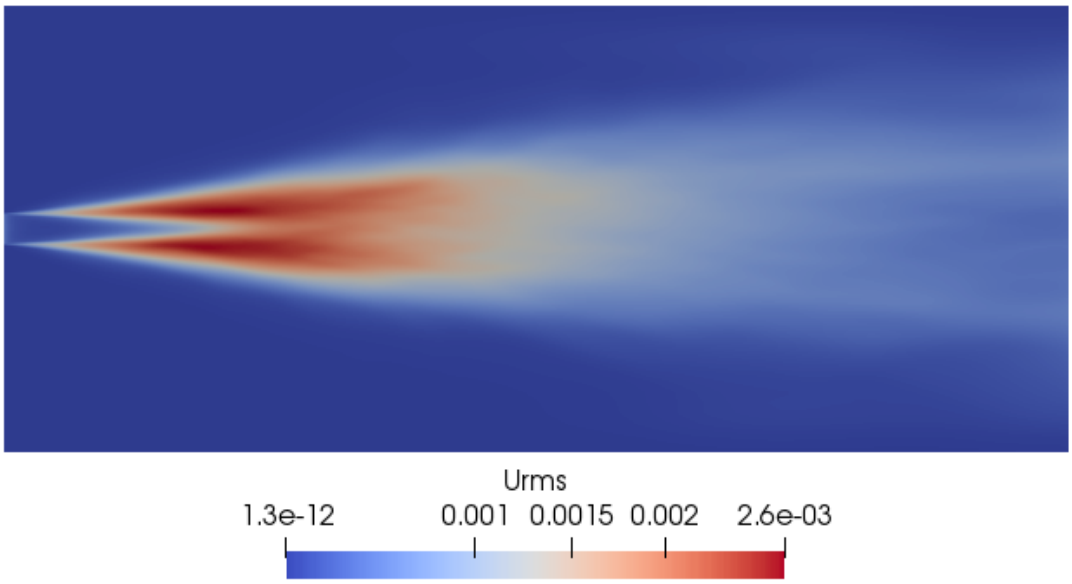

Figure 2.2: Time and spanwise averaged profile of <u'u'>

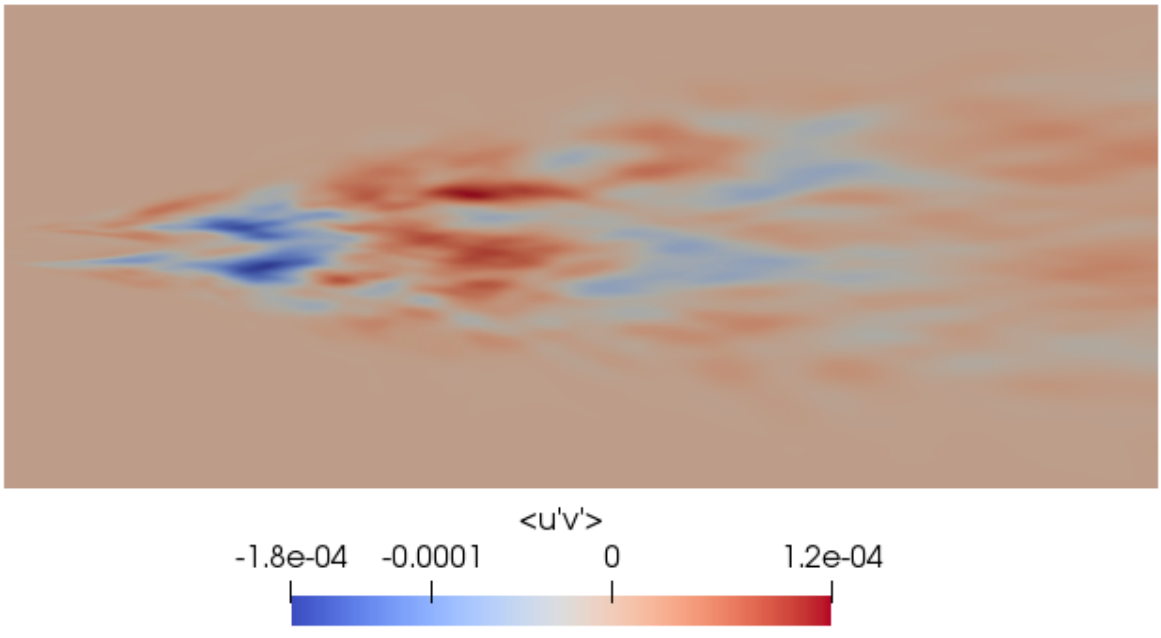

Figure 2.3: Time and spanwise averaged profile of <u'v'>

Evolution of the mean flow:

Transverse profiles of the longitudinal velocity are presented in Figure 2.4. The y direction is normalised by the local jet half width $\delta_{0.5}$ and the time and spanwise averaged jet velocity normalised by the centreline value U_c.

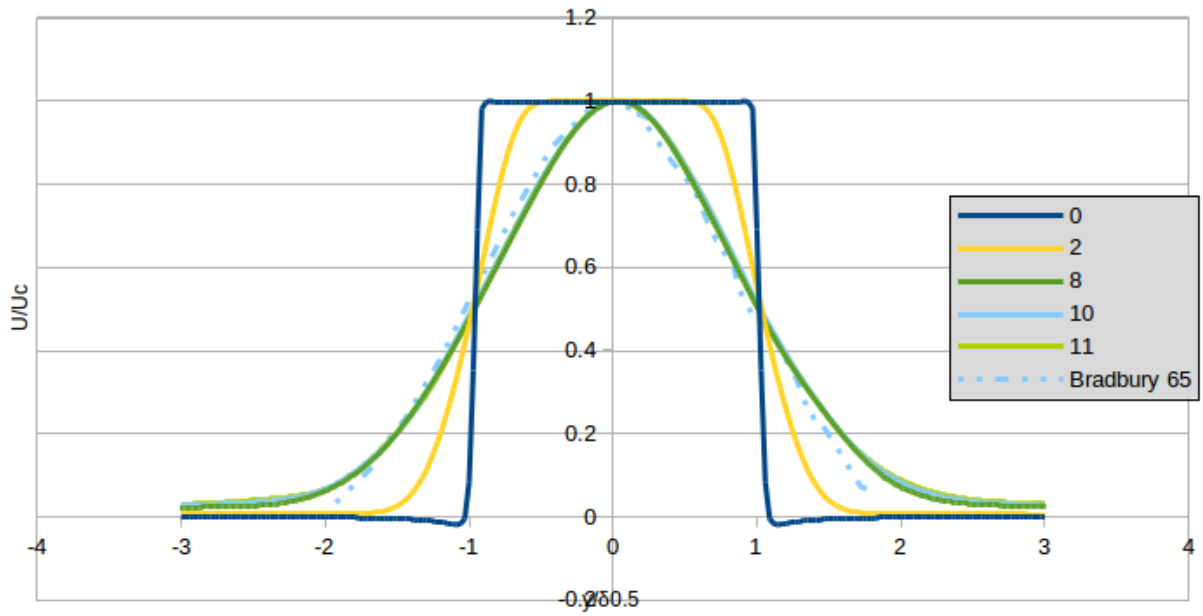

Figure 2.4: Transverse profiles of the longitudinal velocity

The longitudinal mean velocity profile at the inlet is flat, but for the random fluctuations, and then develops rapidly to self-preserving profiles. It can be observed that for x=2d, the jet is not yet self-preserving, but for x>8d, the jet is both self-preserving and agrees well with experimental results. [5].

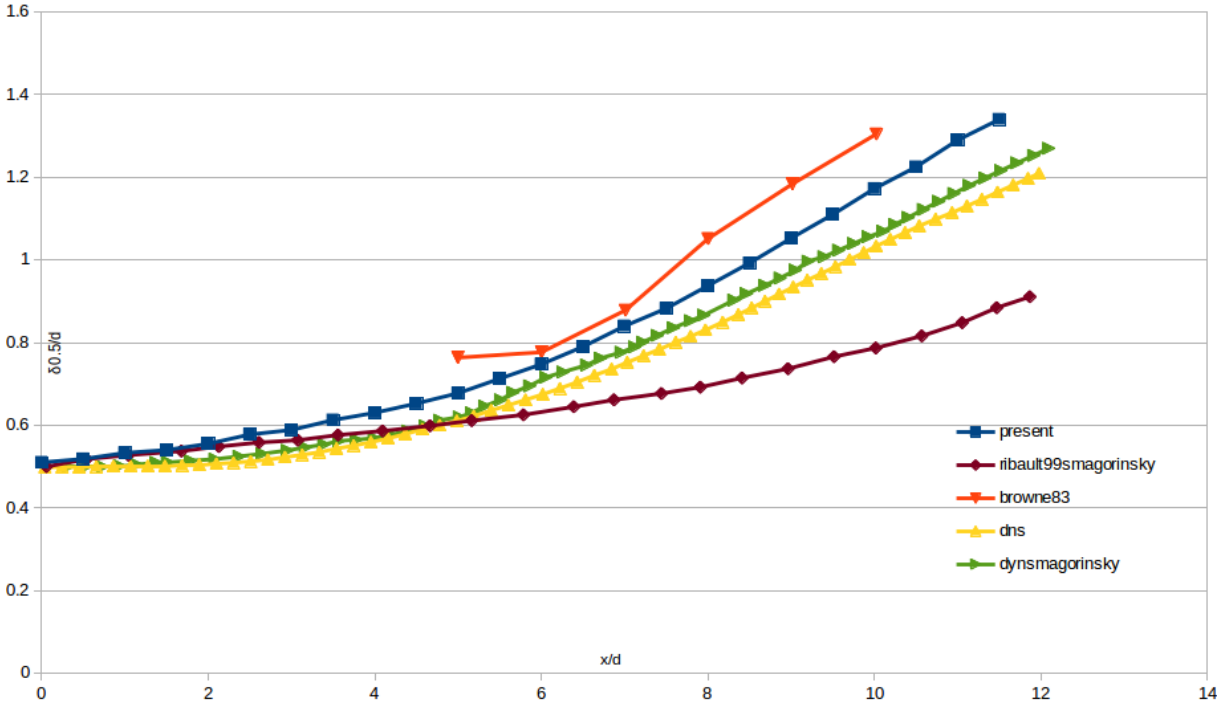

Figure 2.5: Longitudinal evolution of the jet half width

The downstream evolution of the jet half-width is now presented in figure 2.5, along with the DNS and LES results of Ribault, Sarkar, and Stanley[4] and the experimental data from Thomas and Chu[6] for a jet of Re = 8300 and from Browne et al[7] for a jet of Re = 7620. The present simulation is found to closely match the results from literature.

The self-similar behaviour of the jet half width can be fitted to $\delta_{0.5} = K_1 d(x/d + K_2)$. In the region 7<x/d<12, Ribault, Sarkar, and Stanley[4] have reported the DNS evolution to give values of $K_1 = 0.094$ and $K_2 = 0.904$. They also report values of $K_1 = 0.094$ and $K_2 = 1.38$ for LES with a dynamic Smagorinsky model and $K_1 = 0.106$ and $K_2 = 0.4$ for LES with a dynamic mixed model. In experiments K_1 is found to vary between 0.1 and 0.11. The present study finds an approximate value of 0.114 for K_1 and 0.28 for K_2 for the case of 10% fluctuations.

Comparison of Turbulence Intensities:

The downstream evolution of u_{rms} is presented in Figure 2.6. The LES results of Ribault, Sarkar, and Stanley using both the Smargorinsky and the dynamic Smagorinsky models, along with the experimental results of Thomas and Chu, and Browne et al. are also shown for comparison.

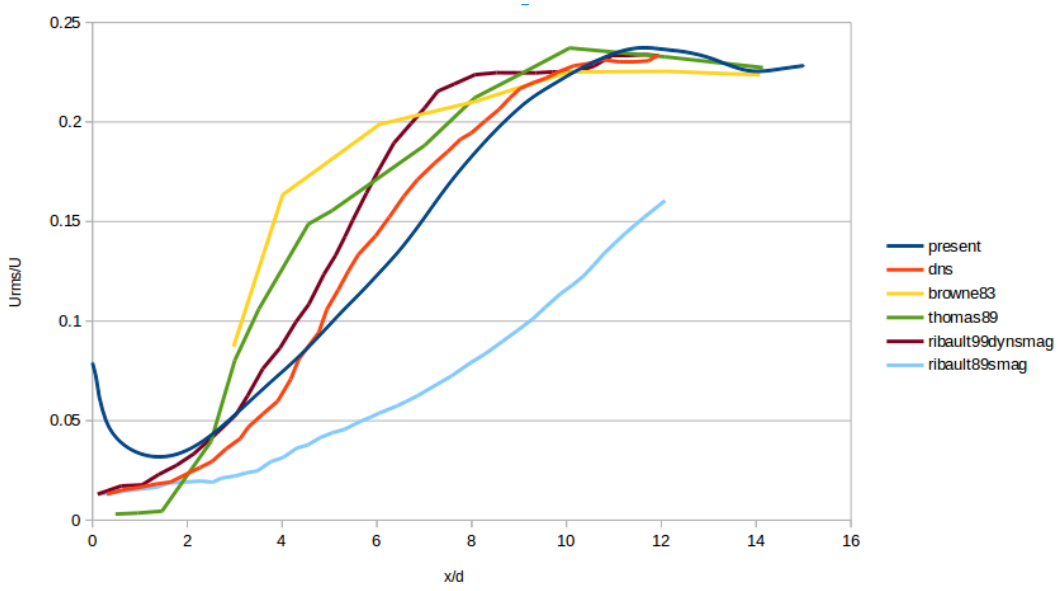

Figure 2.6: downstream evolution of Urms

The profile of the fluctuation intensity u_{rms} at the section x = 11d is compared with the DNS and the Dynamic Smagorinsky LES simulations of Ribault, Sarkar, and Stanley in Figure 2.7. Experimental results by Ramaprian and Chandrasekhara[8] , and Gutmark and Wygnanski are also plotted for comparison.

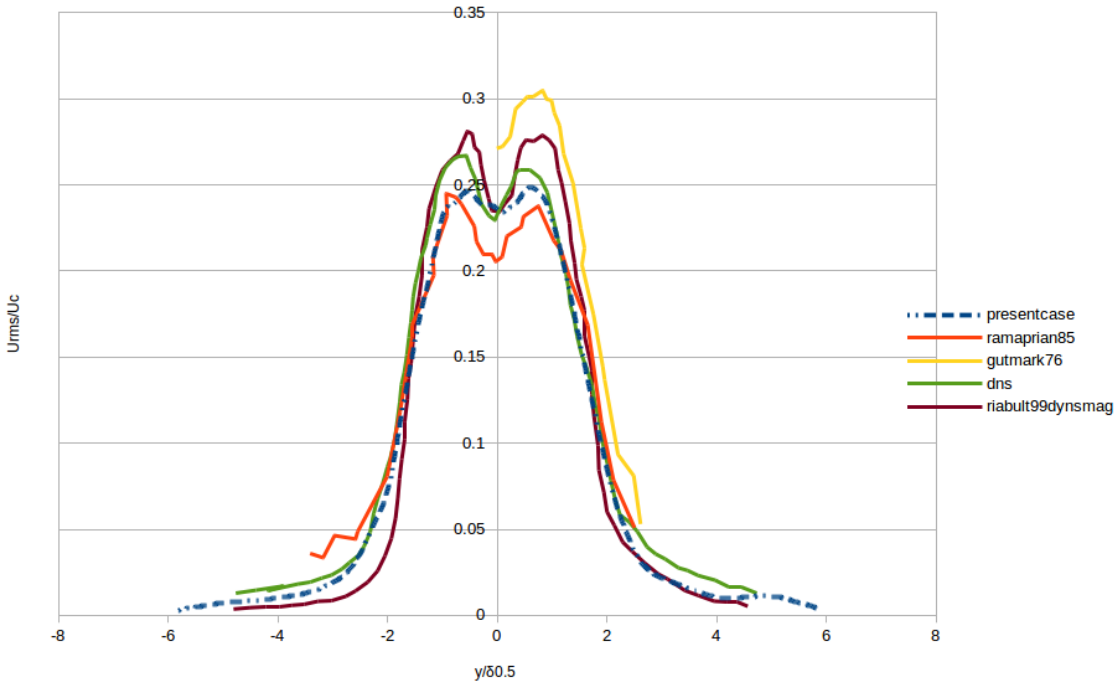

Figure 2.7: Transverse profiles of the rms velocity

The variation of $< u'v' >$ in the longitudinal direction is plotted in figure 2.8.

Figure 2.8: Longitudinal profile of <u'v'>

CHAPTER 3

RANDOM FLUCTUATIONS: 20 PERCENT

3.1 Introduction:

In this case, the magnitude of the inlet fluctuations is equal to 20 percent of the plane inlet jet velocity. Both the velocity U and the fluctuation quantities reported here have been time averaged. The time averaging is done from t=6s to t=18s. Thus obtained time averaged quantities are further averaged in the spanwise direction using the ViSiT software.

3.2 Results:

The time and spanwise averaged velocity profile is shown in Figure 3.1:

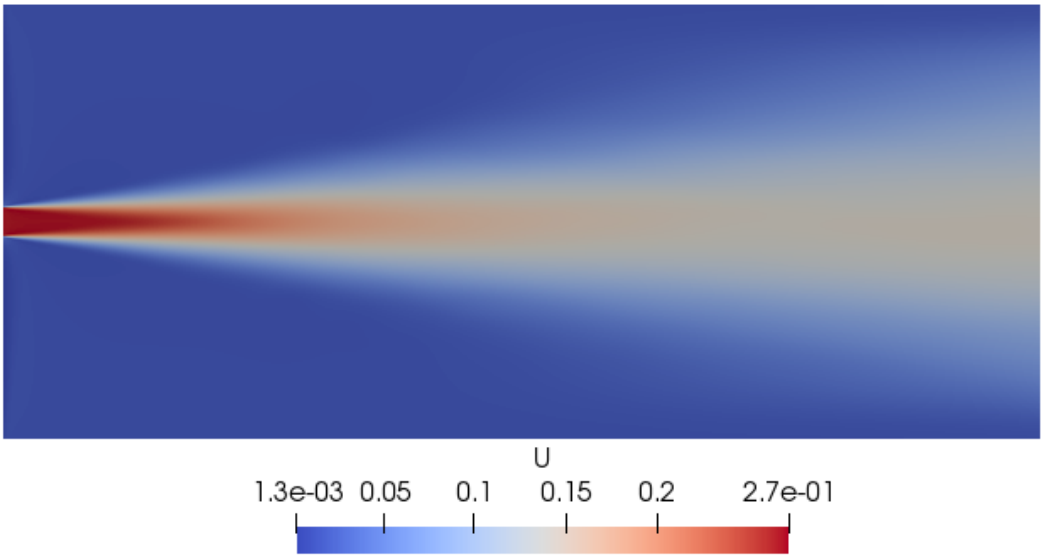

Figure 3.1: Time and spanwise averaged velocity profile

The time and spanwise averaged profiles of $< u'u' >$ and $< u'v' >$ are shown in figures 3.2 and 3.3 respectively. $< u'u' >$ is found to be symmetrical about the centreline, with peaks a small distance away from the centreline.

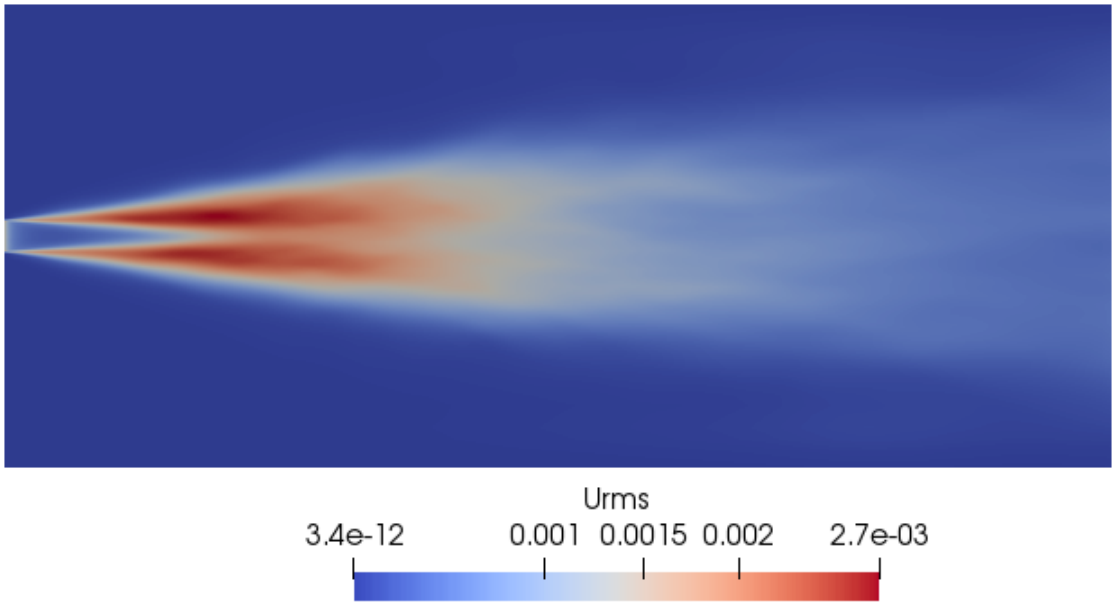

Figure 3.2: Time and spanwise averaged profile of <u'u'>

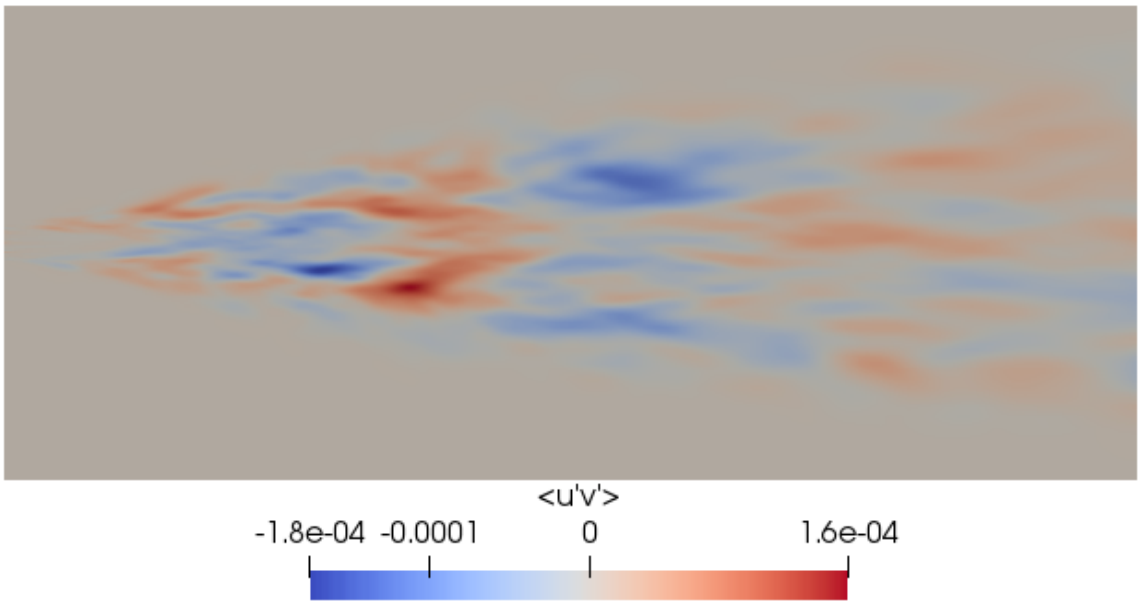

Figure 3.3: Time and spanwise averaged profie of <u'v'>

Figure 3.4 presents the transverse velocity profiles for values of x/d = 0,2,8,10 and 11 comparing them with the experimental results, as well as the DNS and LES results of Ribault, Sarkar, and Stanley as was done for the case with 10% fluctuations. Figure 3.5 shows the longitudinal evolution of the jet half width, compared with results from literature.

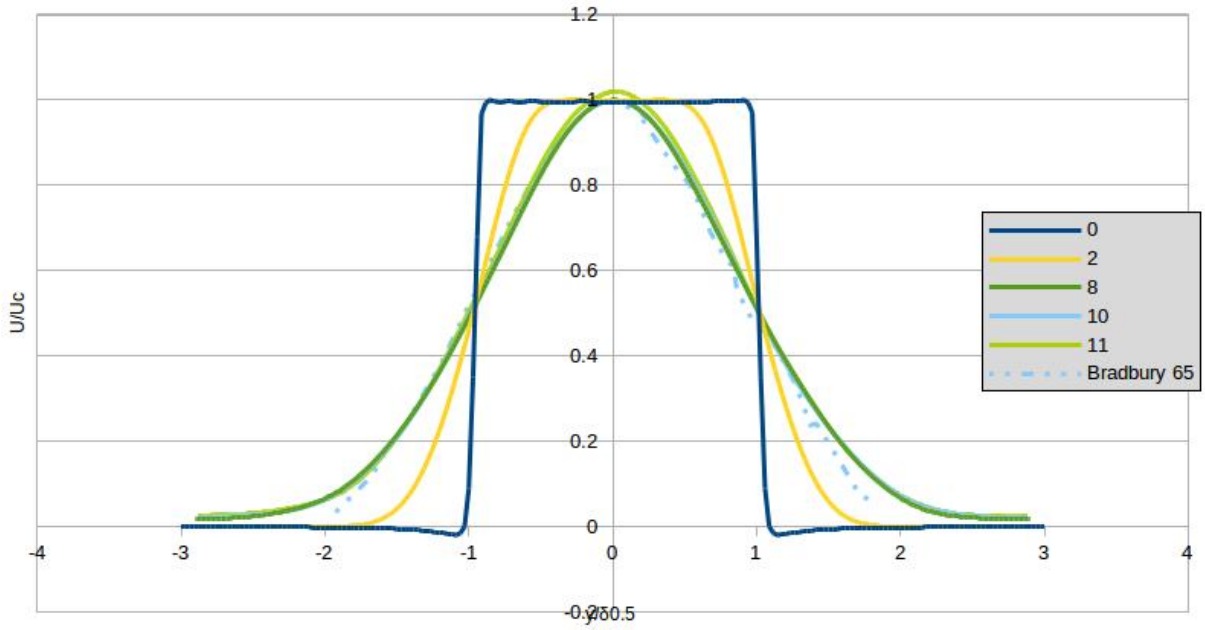

Figure 3.4: Transverse velocity profiles

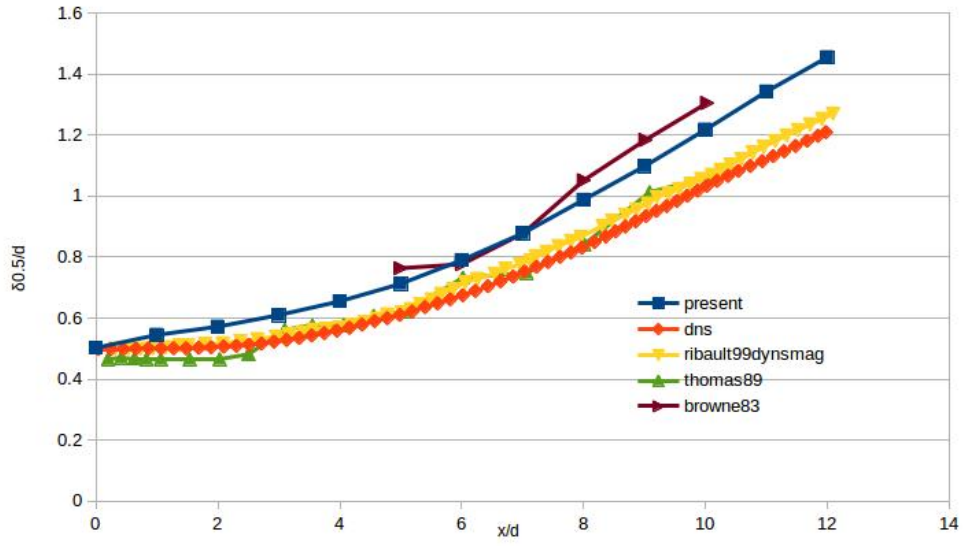

Figure 3.5: Longitudinal evolution of the jet half width

Figure 3.6 compares the longitudinal evolution of the jet half width for the cases with 10% and 20% fluctuations. It is found that the jet spreads quicker when more fluctuations are provided. In the case of 20 percent fluctuations, K_1 is found to be approximately 0.116 and K_2 as 0.5.

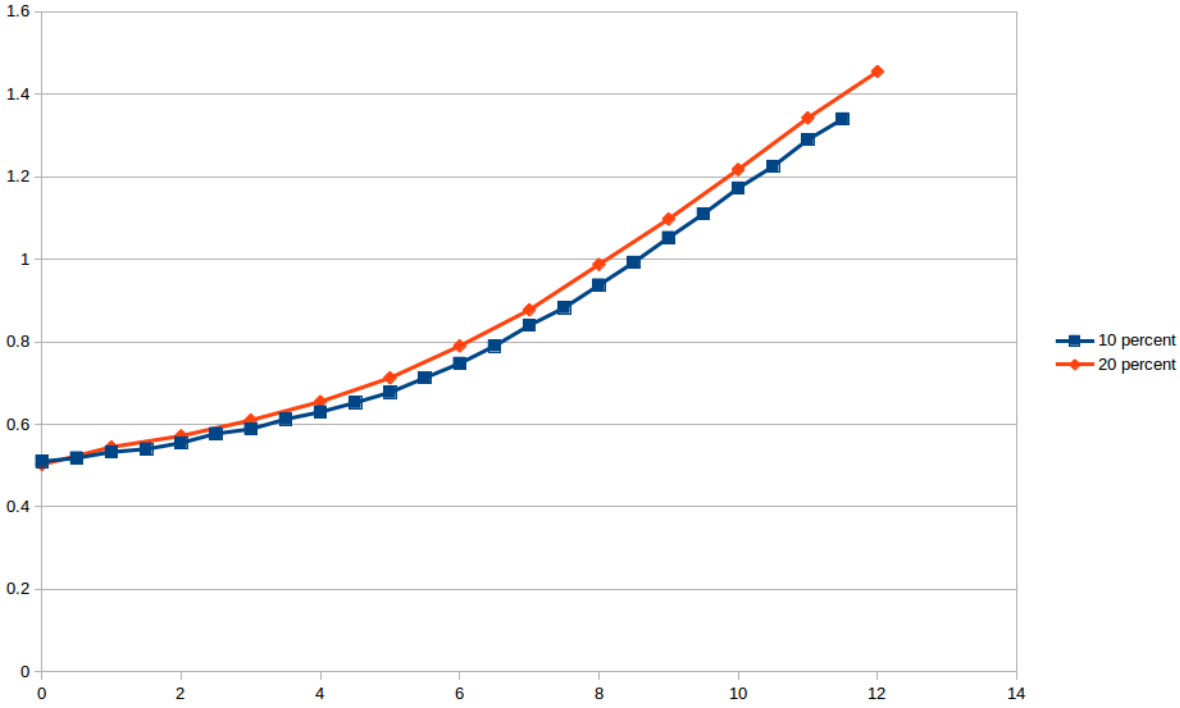

Figure3.6: Longitudinal evolution of the jet half width compared

CHAPTER 4

5 PERCENT FLUCTUATIONS AND COMPARISONS

4.1 Introduction:

In this case, the magnitude of the inlet fluctuations is equal to 5 percent of the plane inlet jet velocity. Both the velocity U and the fluctuation quantities reported here have been time averaged. The time averaging is done from t=6s to t=18s. Thus obtained time averaged quantities are further averaged in the spanwise direction using the ViSiT software.

4.2 Results:

The time and spanwise averaged velocity profile is shown in figure 4.1:

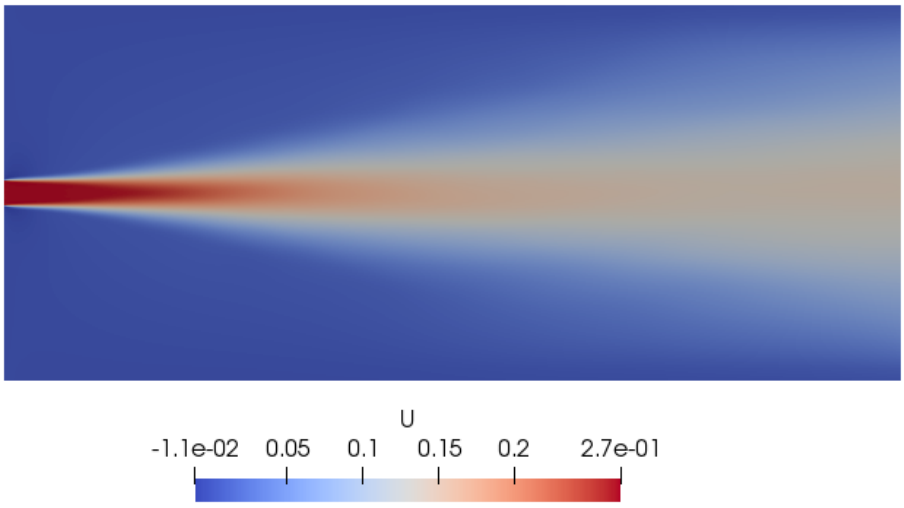

Figure 4.1 : Time and spanwise averaged velocity profile

The time and spanwise averaged profiles of $< u'u' >$ and $< u'v' >$ are shown in figures 4.2 and 4.3 respectively. $< u'u' >$ is found to be symmetrical about the centreline, with peaks a small distance away from the centreline. $< u'v' >$ is not entirely symmetrical because of the presence of the entraining flow in the y-direction.

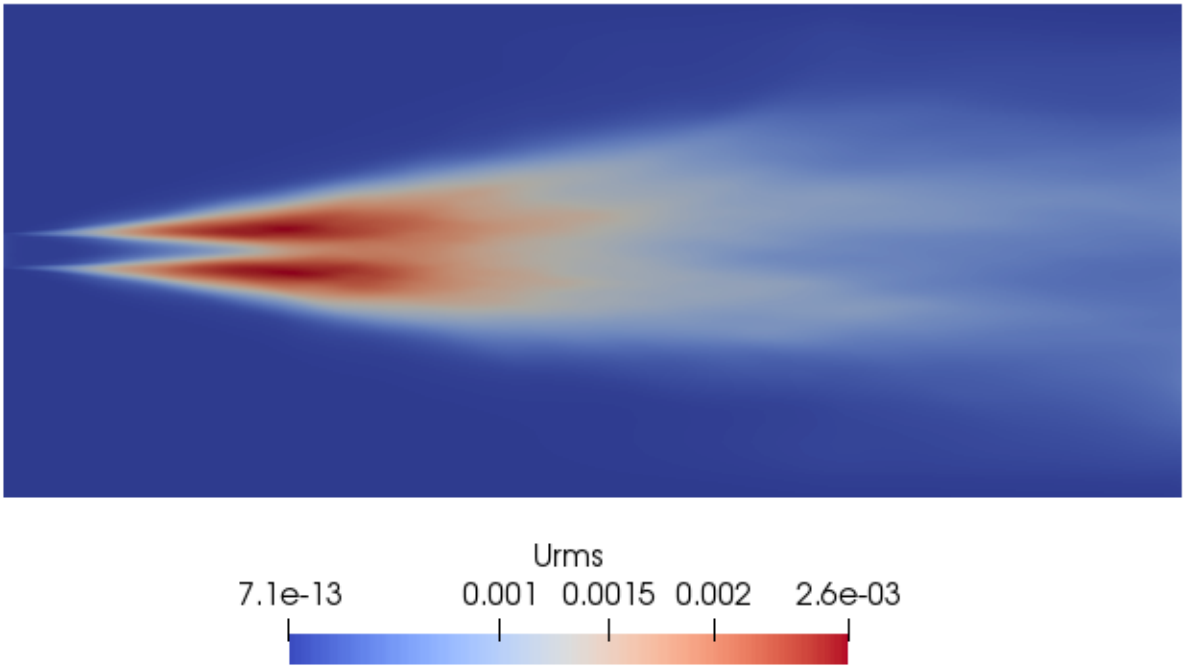

Figure 4.2: Time and spanwise averaged profile of <u'u'>

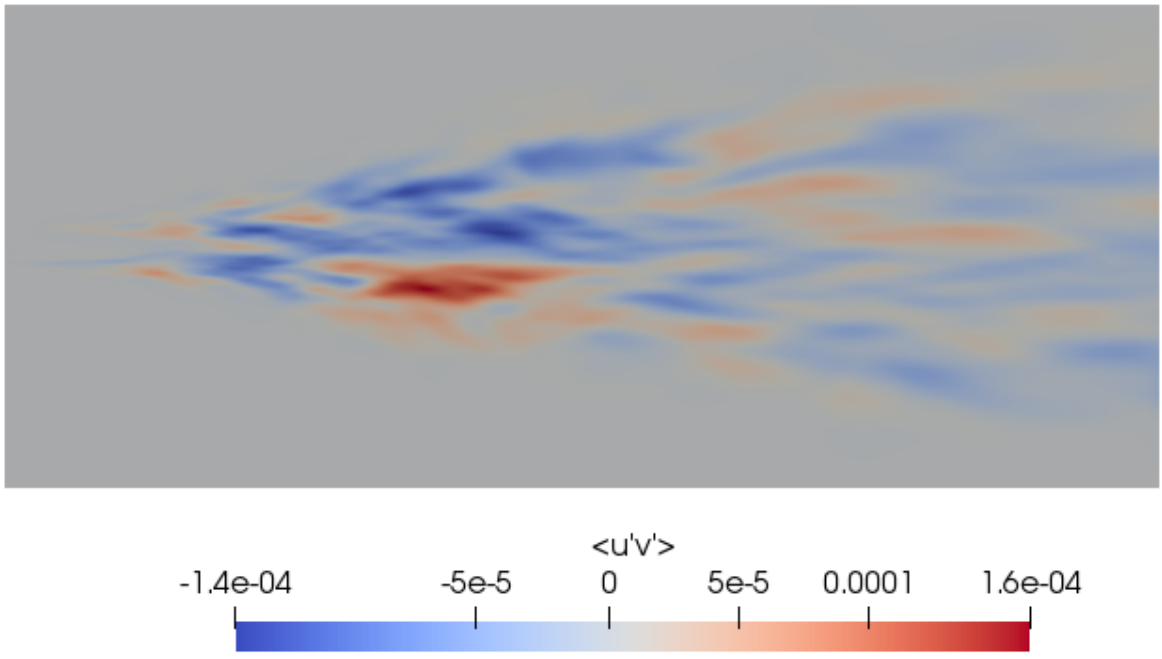

Figure 4.3: Time and spanwise averaged profile of <u'v'>

Figure 4.4 presents the downstream evolution of the jet half width, comparing them with the experimental results, as well as the DNS and LES results of Ribault, Sarkar, and Stanley. In the case of 5 percent fluctuations, K_1 is found to be approximately 0.117 and K_2 as 0.44

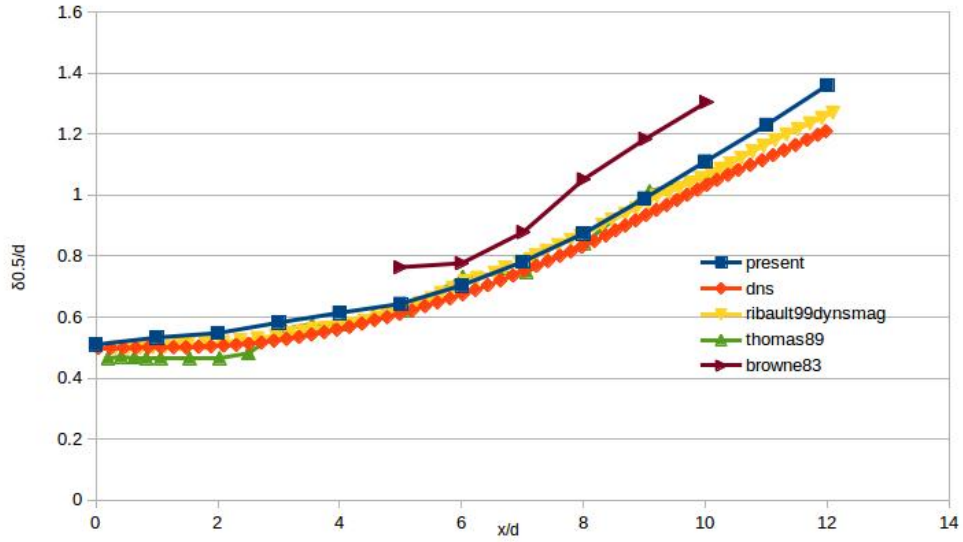

Figure 4.4: Downstream evolution of the jet half width

Figure 4.5 compares the downstream evolution of the jet half width for the 5% case compared ywith the cases with 10% and 20% fluctuations. It is found that the jet spreads quicker when more fluctuations are provided.

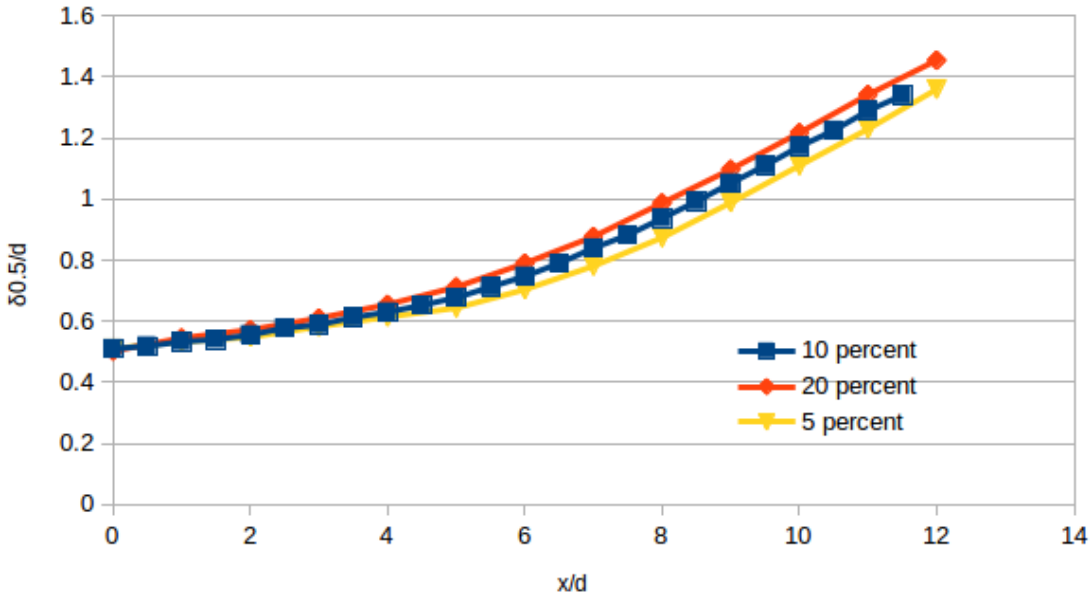

Figure 4.5: Longitudinal evolution of the jet half width compared

Figure 4.6 compares the self similar profiles at x = 11d for 5,10, and 20 percent fluctuations

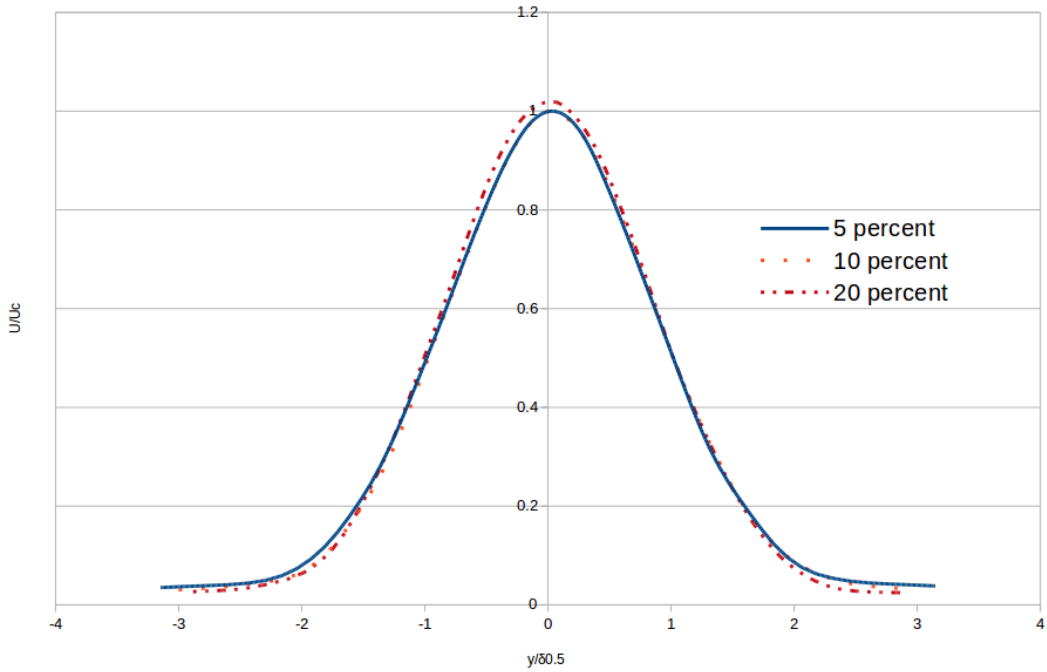

Figure 4.6: Averaged velocity profiles at x = 11d compared for the three different cases

Figure 4.7 compares the evolution of the normalised U_{rms} at the centreline of the jet for the cases considered. Towards the beginning, one sees that higher the inlet fluctuations, higher the U_{rms}.

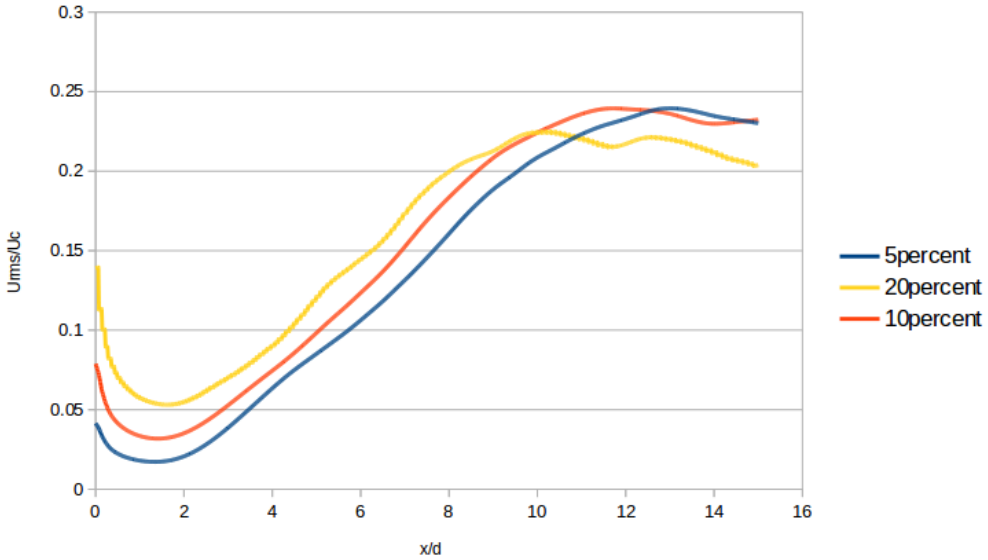

Figure 6: Comparison of evolution of centerline fluctuations

CHAPTER 5

CONCLUDING REMARKS AND SCOPE FOR FUTURE WORK

5.1 Concluding Remarks

The random fluctuations method has been studied for the case of a plane jet using OpenFOAM. The turbulence characteristics of all three cases of the plane jet studied, ie., with 5%, 10%, and 20% fluctuations are found to approximately match the DNS and experimental results. It is found that increasing fluctuations causes the jet to start spreading a bit earlier.

5.2 Grid Independence for LES

Since the length scale in LES is dependent on the gird size(for example, for the simulations presented here, the cubeRootVol method is used. ie., $\Delta = c(V_c)^{\frac{1}{3}}$.), LES is inherently not grid independent.

We have considered a finer mesh with 1.552 million cells and compared the longitudinal evolution of turbulent fluctuations with the case with 10% fluctuations. Averaging has been done from t=6s to t=9.5s. Spanwise averaging is done using VisIt The result is presented in Fig. 5.1.

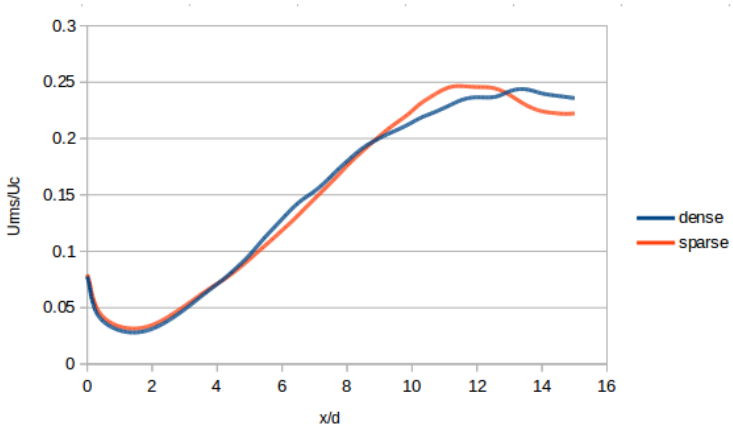

Figure 5.1 : Denser and coarser grids compared

5.3 Synthetic Eddy Method and Divergence Free Synthetic Eddy Method

The synthetic eddy method works by simulating eddies in a box extruding from the inlet and using these eddies to calculate $\boldsymbol{u}'$ to superimpose on the (user defined)inlet velocity. The formula proposed for u' by Jarrin et al[13]. is:

$$u_i'(x) = \frac{1}{\sqrt{N}} \sum_{k=1}^{N} a_{ij} \varepsilon_j^k f_\sigma^k \left(\frac{x - x^k}{\sigma^k} \right)$$

Where N is the number of eddies introduced into the SEM domain; x^k is the location of the kth eddy; σ^k is the turbulent length scale calculated at the eddy centre; f is a suitable shape function; ε_j^k are random numbers with zero average and $\langle \varepsilon_j^k \varepsilon_j^k \rangle = 1$; and a_{ij} are the Lund coefficients defined in Lund et al.[12] and written as

$$a_{ij} = \begin{bmatrix} \sqrt{R_{11}} & 0 & 0 \\ \frac{R_{21}}{a_{11}} & \sqrt{R_{22} - a_{21}^2} & 0 \\ \frac{R_{31}}{a_{11}} & \frac{R_{32} - a_{22} a_{31}}{a_{22}} & \sqrt{R_{33} - a_{31}^2 - a_{32}^2} \end{bmatrix}$$

Where R_{ij} is the Reynolds stress tensor. However, the disadvantage of this method is that the velocity field is not usually divergence free, which is unphysical as it violates the Navier-Stokes equations.

A Divergence free synthetic eddy method has been proposed by Poletto et al.[10]

5.4 Digital Filter Method:

The digital filter method works by creating velocities from random data using a digital filter.

$$u_m = \sum_{n=-N}^{N} b_n r_{m+n}$$

Where b_n is the filter coefficient and r_m is a series of random numbers with zero mean and an rms value of 1.

Because $\overline{r_m r_n} = 0$ the filter coefficients can be linked to the correlations as:

$$\frac{\overline{u_m u_{m+k}}}{u_m u_m} = \sum_{j=-N+k}^{N} b_j b_{j-k} \Big/ \sum_{j=-N+k}^{N} b_j^2$$

A three dimensional filter is obtained by the convolution of three one dimensional filters.

$$b_{ijk} = b_i . b_j . b_k$$

Klein, Sadiki, and Janicka[9]have proposed a digital filter method where the filter coefficients are given by:

$$b_k \approx \frac{\tilde{b}_k}{\sqrt{\sum_{j=-N}^{N} \tilde{b}_j{}^2}} \text{ and } \tilde{b}_k \coloneqq \exp\left(\frac{-\pi k^2}{4n^2}\right)$$

REFERENCES

[1] X. Wu, “Inflow turbulence generation methods Annual Reviews”, 2017

[2] Lewis F Richardson, **“**Weather prediction by numerical processes Cambridge University Press”, 1922

[3] Stephen B Pope, **“**Turbulent Flows” Cambridge University Press 2000

[4] C. Le Ribault, S. Sarkar, and S.A. Stanley, **“**Large Eddy Simulation of a plane jet**”** **,**Physics of Fluids, 2001

[5] L.J.S Bradbury, “The structure of a self-preserving turbulent plane jet”, J. Fluid Mech 23(1), pp 31-64, 1965

[6] F.O. Thomas and H.C. Chu, “An experimental investigation of the transition of a planar jet: Subharmonic suppression and upstream feed-back”, Phys. Fluids A. , pp. 1566-1587, 1989

[7] L.W.B. Browne, R.A. Antonia, S. Rajagopalan, and A.J. Chambers, “Interaction region of a two-dimensional turbulent plane jet in still air”, in Structure of Complex Turbulent Shear Flow, eidted by R. Dumas and L. Fulachier IUTAM Symp. Marseille. Springer, New York, pp. 411-419, 1983

[8] B.R. Ramaprian and M.S. Chandrasekhara, “LDA measurements in plane turbulent jets”, ASME Fluids Engg., pp 264-271, 1985

[9] M.Klein, A Sadiki, and J. Janicka, “A digital filter based generation of inflow data for spatially based developing direct numerical or large eddy simulations”, J Computational Physics pp 652-665, 2003

[10] R. Poletto, T. Craft, and A. Revell, “A new divergence free synthetic eddy method for the reproduction of inlet flow conditions for LES”, Flow turbulence and combustion pp. 519-539, 2013

[11] Leonard A., “Energy cascade in large-eddy simulations of turbulent fluid flows” ,Advances in Geophysics A, pp 237-248, 1974

[12] T. Lund, X. Wu, D. Squires, “Generation of turbulent inflow data for spatially developing boundary layer simualtions”. J Comp. Phys. 140, pp 233-258, 1998

[13] Jarrin. N, R. Prosser, J. Uribe, S. Benhamadouche, and D. Laurence, ”Reconstruction of turbulent fluctuations for hybrid RANS/LES simulations using a Synthetic-Eddy method”, International Journal of heat and fluid flow 30(3), pp 435-442, 2009

[14] E. Gutmark and I. Wygnanski, “The planar turbulent jet”, J. Fluid Mech, pp465-495, 1976